Available online at www.sciencedirect.com
ScienceDirect
Ceramics International 38 (2012) 333–340
CERAMICS INTERNATIONAL
www.elsevier.com/locate/ceramint

The growth of SAPO 34 membrane layer on support surface for gas permeation application

Jugal K. Das, Nandini Das *, Soumendra N. Roy, Sibdas Bandyopadhyay

Ceramic Membrane Division, Central Glass & Ceramic Research Institute, CSIR, 196, Raja SC Mullick Road, Jadavpur, Kolkata 700 032, India

Received 4 April 2011; received in revised form 29 June 2011; accepted 6 July 2011
Available online 18th July 2011

Abstract

The formation stage of SAPO 34 zeolite membrane on a tubular mullite support has been investigated. XRD, FESEM, IR and EDAX analysis techniques were used to explain the changes in crystallization stages as well as formation of membrane on tubular clay–alumina support with time. From the studies, the evidence tends to support that crystallization of SAPO 34 started from initial gel, proceed through cluster formation and accumulation followed by segregation and crystallization process. The study also showed the gradual incorporation of Si into $AlPO_4$ phase and form cubical CHA phase after 120 h of synthesis time.

Single gas permeation of CO_2 and H_2 showed that upto 300 KPa of feed pressure permeability of CO_2 is more than that of H_2. But at higher pressure the results show the reverse trend, flux is more for H_2. This may be due to more adsorption of CO_2 on SAPO 34 surface and less desorption from the surface than hydrogen with increasing pressure. The selectivity of H_2/CO_2 increases from 0.85 to 2.67.

Keywords: Zeolite membrane; Single gas permeation; Crystal growth

1. Introduction

In recent years, attempts to develop zeolite membranes for separation and catalytic application have been intensified. Considering their molecular sieving properties and uniform pore size, high thermal resistance, and high mechanical strength, zeolite membrane have attracted great interest for application in many important industrial processes [1,2].

Now a days, hydrogen used as clean energy fuel, are mostly synthesize from CBM gas by WGS reaction and it has to be separated from CO_2, CO, H_2O, etc. [3]. Comparing to other types of separation processes, membrane separation is most suitable for its ease of operation, low energy consumption and also cost effective [4,5]. Zeolite membrane is a potential material for gas separation applications. Among the various types of zeolite species, especially SAPO 34 zeolite has the potential to sieve out CO_2 molecules from a mixture of CO_2/H_2 for water gas shift reaction by molecular sieving interaction, due to its kinetic diameter difference. Hydrogen has a higher diffusivity than any other molecules due to their smaller kinetic diameter. But hydrogen adsorbs weakly comparing to other gas [6] As a result it has been commercially applied to CO_2 removal from H_2 from WGS gas stream [7].

There are many reports on the improvement of the formation stages of the membranes like microwave heating [8], addition of intermediate silane layer to increase the adhesion between gel layer and supporting substrate [9], vacuum seeding [10] etc.

The in situ hydrothermal synthesis appears to be the best studied method, in which the porous support is immersed into the synthesis solution, and then the membrane is formed by direct crystallization. However, it is difficult to prepare high quality membrane by this in situ crystallization method directly [11]. Coating the zeolite seed on the support surface before hydrothermal synthesis, which is also called as secondary growth method, is an effective approach to develop a high quality zeolite membrane. It is well known that the presence of seed on the support surface plays an important role in membrane formation. Synthesis with seeds gives a better controlled of the membrane formation process by separating the crystal nucleation and growth with a shortened crystallization time [12]. In addition, the secondary growth ensures the formation of the phase pure zeolite crystal on the support. The

* Corresponding author. Tel.: +91 33 2483 8082; fax: +91 033 2473 0957.
E-mail address: dasnandini@cgcri.res.in (N. Das).

0272-8842/$36.00
doi:10.1016/j.ceramint.2011.07.011

secondary growth method which was proposed by Lovallo et al. exhibit many advantages such as better control over membrane micro-structure, and higher reproducibility [13].

In this work, SAPO 34 zeolite membrane layer was synthesized on alumina substrate by secondary growth method. Small zeolite crystals were used as nucleation seeds. Almost dense zeolite membrane was synthesized on properly seeded substrate. Gradual formation stages of membrane layer with time on support surface were studied. The synthesized zeolite and membrane was characterized using XRD, FESEM, EDAX and TEM. The ultimate performance of the membrane was characterized by gas permeation measurement.

2. Experimental

The SAPO 34 membrane was synthesized by ex situ crystallization on a porous alumina tube of diameter 10 mm and thickness 3 mm and 60 mm length (prepared in our laboratory from clay–alumina mixture, used as substrate). Before coating, the substrates were cleaned with acetone in an ultrasonic cleaner (vibracell, USA) for 5 min just to remove dust particles and oily matter. The outer surface of the cleaned substrates was wrapped with Teflon tape. The inside of the tube samples was coated with aqueous solution of zeolite seeds. The seed layer was applied by dip coating method.

In order to get a uniform seed layer on the support surface, the seeds should be dispersed homogeneously on the support surface and amount of nucleation seeds should not be too large otherwise the membrane layer will be too thick and uneven.

In this nucleation seeds coating process, the support substrate were dipped in a 1–3% SAPO 34 zeolite seed suspension in deionized water, for different time span ranging from 5 times to 10 times with a duration of 15 s. After the dipping procedure, the seeded supports were dried at 100 °C for 24 h.

The SAPO 34 membrane layer was synthesized hydrothermally on porous modified, seeded support tubes. The materials used for the synthesis were boehmite powder (SASOl), silica sol (Ludox 40 AS), phosphoric acid (Qualigens Fine Chemicals, India) and morpholine (Sd fine chemicals, India), and distilled water. Two reactant mixtures were prepared respectively dissolving boehmite powder and phosphoric acid and required amount of water (mixture 1) to the reaction mixture. The mixture was stirred for overnight. In another mixture (mixture 2) silica sol and morpholin was added and rest amount of water was added to the reaction mixture. After stirring the mixture 2 for 1 h, it was mixed slowly under stirring at room temperature to mixture 1. The resulting mixture was stirred vigorously for 15–30 min and kept under stirring for overnight to produce a homogeneous sol. The molar composition of the sol used for the synthesis was Al_2O_3:SiO_2:P_2O_5:H_2O 1:0.3:1:66. The seeded substrate was placed vertically in an autoclave. Crystallization was continued under autogenous pressure in a hot air oven at 170–175 °C for 48–120 h. Repeated crystallization for second stage and third stage was carried out to improve the quality of the membrane. After synthesis, the zeolite coated membrane was washed thoroughly with deionized water until the pH of the washing liquid became neutral. The crystalline structure of the as synthesized membrane was determined by XRD pattern. XRD was carried out on a Philips 1710 diffractometer using CuK_α radiation (α = 1.541 Å).

Microstructure and morphology of the growth layer was examined using scanning electron microscopy (FESEM: model Leo, S430i, UK). Single gas and mixture gas permeation for H_2 and CO_2 were measured by a specially designed permeation cell developed in our laboratory. A solid tube was used instead of membrane tube to check the seal of the system. The gas permeance of the membranes was measured by soap film flow meter under the feed pressure of 200–500 kPa and at room temperature. The permselectivity of two single gases G_1/G_2 was defined as the permeance ratio of G_1 and gas G_2. The gas permeation measurement of each single gas was repeated until the permeance data for the successive 10 tests were closed. The single gas permeance was the average of 10 successive tests. In case of mixture gases, equimolecular amount of two gases CO_2

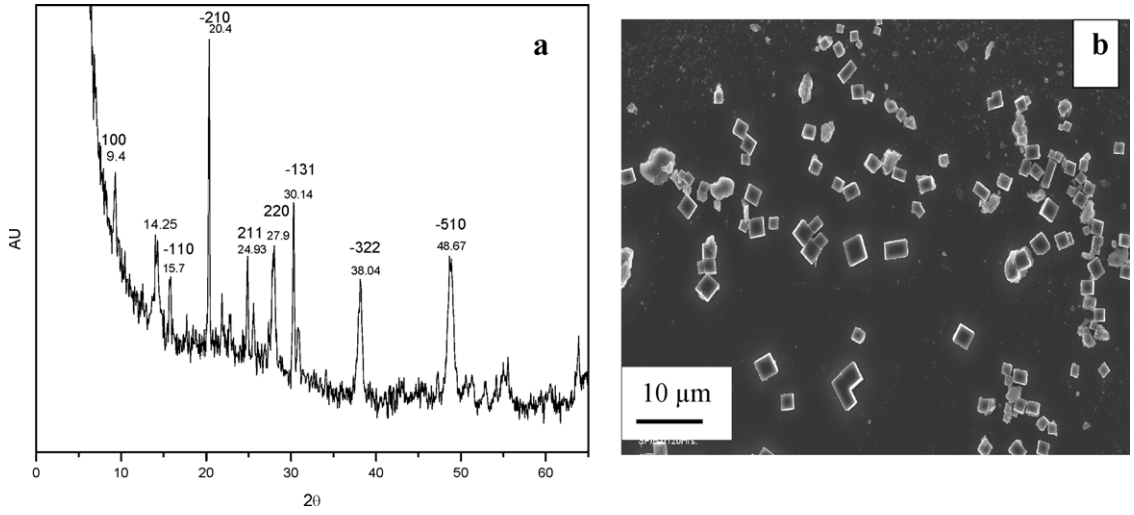

Fig. 1. (a) XRD pattern and (b) FESEM of SAPO 34 crystals used as seed for membrane synthesis.

and H_2 were mixed through mass flow controller. The composition of the feed and permeate streams were measured by gas chromatograph. Selectivity is defined as the permeance of each gases of the mixture.

3. Results and discussion

In order to form a continuous zeolite membrane on the support surface, the nucleation of zeolite in the bulk synthesis mixture must be inhibited, while the nucleation of zeolite on the support surface must be increased. According to the formation mechanism of zeolite membrane on the porous support, the nucleation of zeolite on the support/gel interface and in the bulk synthesis mixture are competitive processes [14]. So, in this work, all the membrane synthesis was done by ex situ method. Thus, in case of synthesis of continuous membrane layer, seed crystals must be added before synthesis. Fig. 1 depicts the XRD, FESEM image of SAPO 34 crystals used as seed for synthesis of membrane. Comparing the XRD and FESEM, the size range of seed crystals, are 1–5 μm.

Fig. 2 shows the XRD pattern of SAPO 34 membrane synthesized for 48 h, 72 h, 96 h and 120 h and compared with standard pattern of SAPO 34 zeolite. As the diffraction intensity of the SAPO 34 zeolite membrane on support surface was too weak to detect by XRD, the diffraction pattern of the bulk powders collected from hydrothermal container were studied. It is clear from the XRD pattern that after 48 h of synthesis some crystalline phase was started to form and continues upto 72 h.but the phase was not SAPO 34. After prolonged heating, at 96 h, the crystalline phase was converted into amorphous phase and on further heating, it was transformed into SAPO 34 after 120 h. All SAPO 34 synthesis employed morpholine as a template.

The DTA/TGA pattern of SAPO 34 membrane synthesized for different time ranges from 72 h to 120 h are shown in Fig. 3. It is clear from the figure that in three cases weight loss upto 200 °C is 8% and it was may be due to adsorbed moisture and

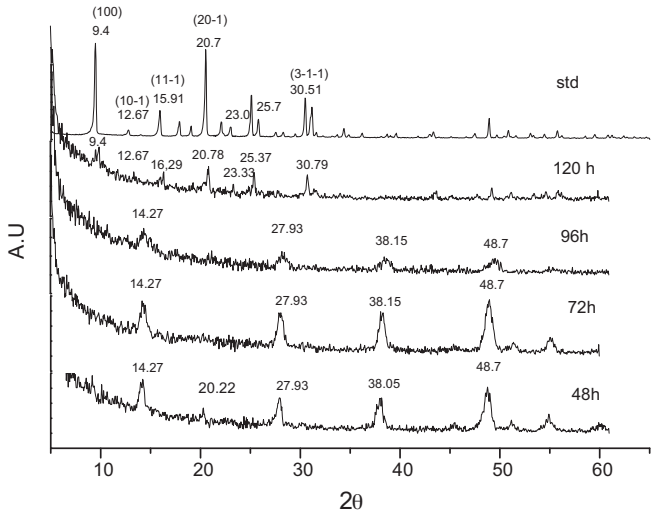

Fig. 2. XRD pattern of SAPO 34 crystals synthesized for different time ranging from 48 to 120 h.

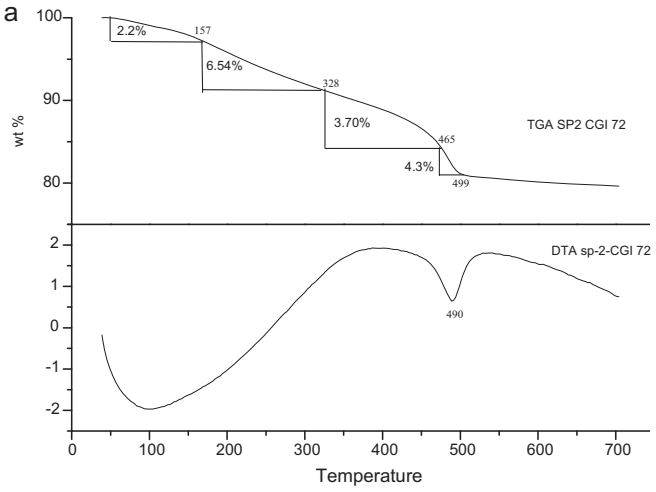

DTA TGA curve for 72h

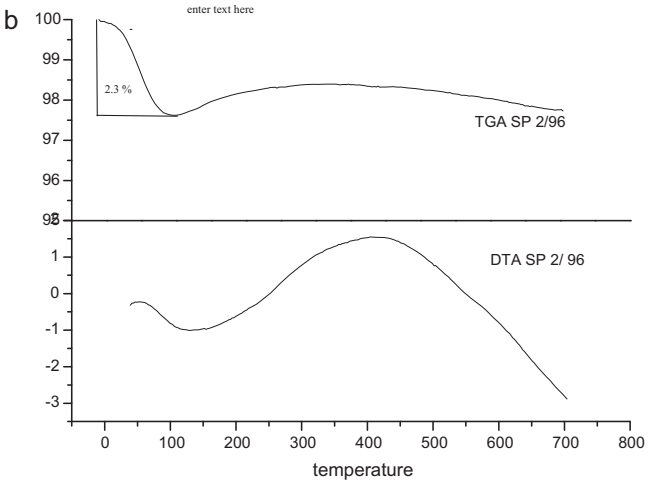

DTA TGA curve for 96h

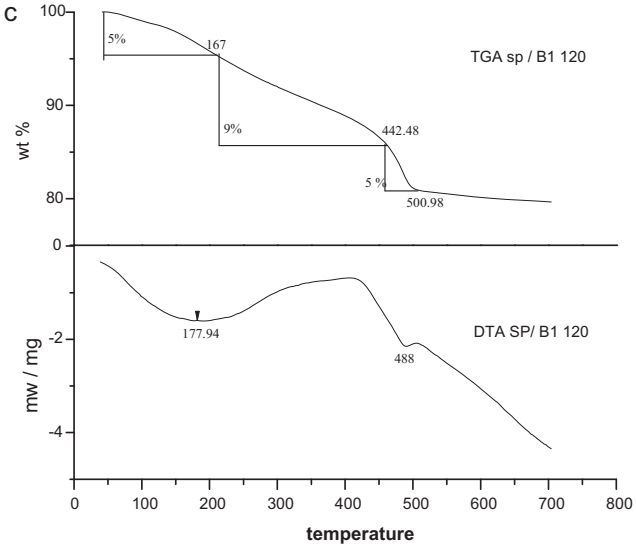

DTA TGA curve for 120h

Fig. 3. DTA TGA pattern of SAPO 34 powders.

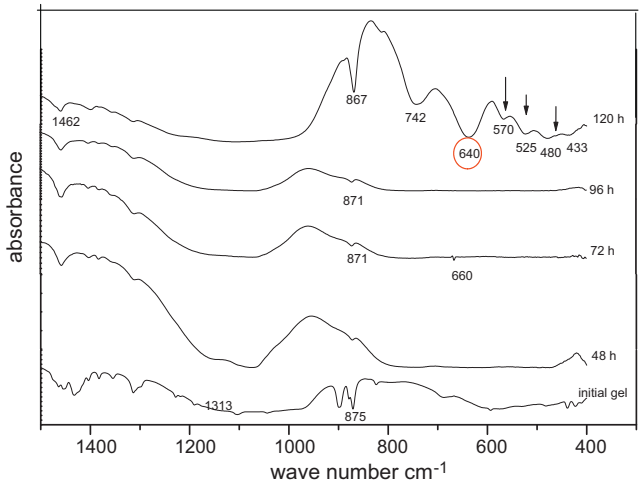

Fig. 4. IR Spectra of zeolite samples synthesized at different time ranging from 0 (initial gel mixture) to 120 h.

mass loss above 350–500 °C is attributed to decomposition of entrapped morpholin in the pore cage of synthesized zeolite. For samples synthesized for 72 h the weight loss due to morpholin was 8% and for 96 h, it was almost zero and for 120 h synthesized powder, the value is 14%.

As described earlier that during hydrothermal process, upto 72 h different phase of SAPO 34 was formed. After prolonged heating the zeolite sample lost its crystallinity and structure beaks down to amorphous phase and as a result, no entrapped morpholin was there and weight loss due to morpholin in this case is zero. This observation was supported by IR analysis of the same samples as described in Fig. 4.

Fig. 4 depictes the IR spectra of the samples synthesized for different time. The characteristics band at 480, 534, and 640 are observed for 120 h synthesized samples and they represent the vibration corresponding to SiO_4, $(Si,Al)O_4$, PO_4 and D-6 rings respectively [15] and it confirms the formation of SAPO 34 with CHA structure. From this it is clear that only after 120 h full grown zeolite structure is obtained.

As we discussed, from XRD pattern, after prolonged heating upto 96 h, the ''pseudo crystalline'' structure was destroyed and some amorphous phase was formed. Then further heating by hydrothermal process, the amorphous phase was recrystallized to form SAPO 34 phase. All samples were not properly crystalline as shown by the FESEM images in Fig. 5. But the properly crystalline structure appeared to be cubic, reflecting the rhombohedral symmetry of the CHA structure.

EDX-analysis of SAPO 34 as a function of synthesis time are described in Table 1 synthesis time and again increases upto

Table 1
Elemental analysis of different stages during the synthesis of SAPO 34.

Sample	Time of crystallization	Al	P	Si
SA 1	15 h	3.59	92.33	4.05
SA 2	30 h	47.00	38.21	14.79
SA 3	96 h	89.79	3.19	7.04
SA 4	120 h	52.86	32.70	14.42

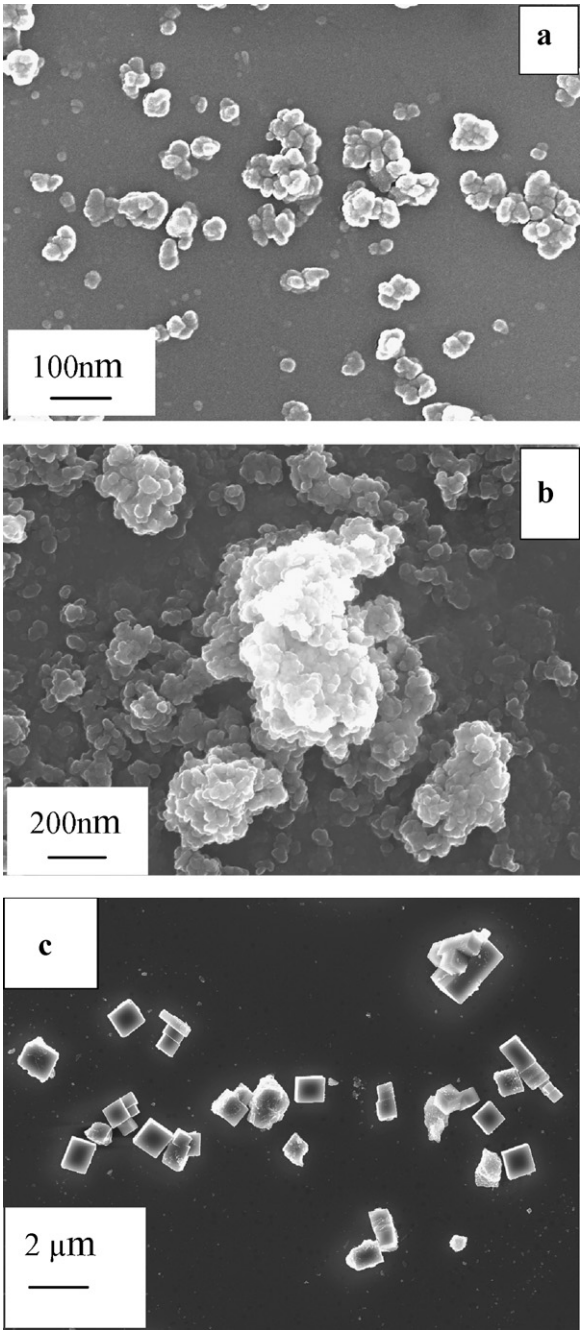

Fig. 5. FESEM images of SAPO 34 powders synthesized for (a) 48 h, (b) 96 h, (c) 120 h.

120 h where SAPO 34 of CHA structure was formed as attributed from IR spectra.

At initial stage, the maximum amount of phosphorus was detected. More interestingly, the amount of Si increased with synthesis time at the expense of the P, with increasing time upto 30 h. As expected from the silicon substitution mechanisms in $AlPO_4$ proposed by Ashtekar et al. [16] (the major part of the Si substitutes isolated phosphorus atoms, as a results the large reduction was observed for the phosphorus atom. But after 96 h of synthesis, Al atom content increases and P atom content decreases drastically. These general trends are interesting because control of the synthesis times might be applied to

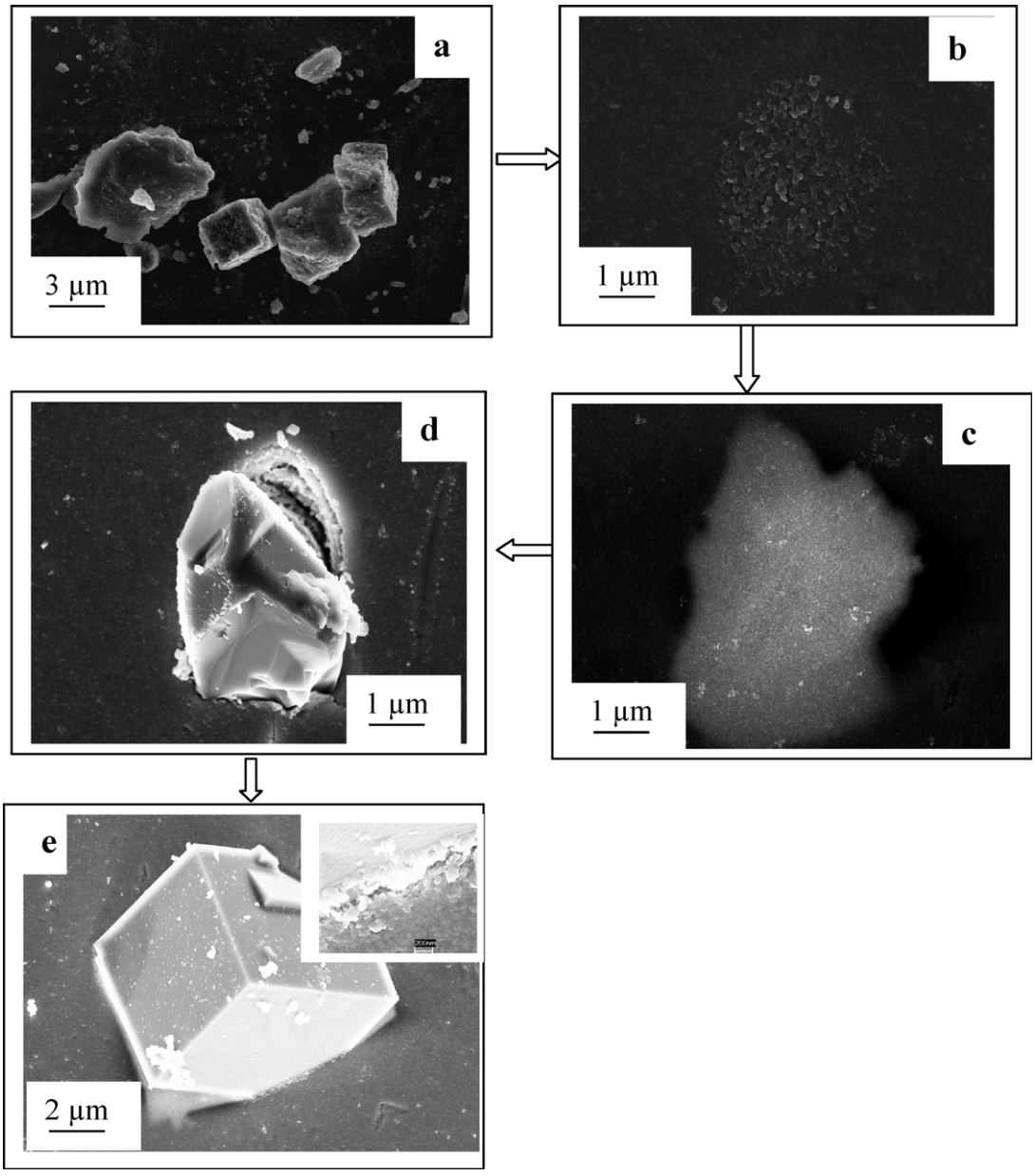

Fig. 6. Gradual formation of zeolite crystals between 48 h and 120 h (a) 48 h, (b, c) 72 h, (d) 96 h, (e) 120 h (inset shows the interface between gel layer and crystal face).

control the silicon content in the final product. As we observed after 120 h of synthesis, silicon content increases and complete crystallization of SAPO 34 was observed. Fig. 6 describes the gradual formation of zeolite crystal from initial gel. In initial stage, cluster accumulation and segregation was occurred (Fig. 6a and b). Then gradual crystallization continues until cubic crystalline chabazite structure is formed (Fig. 6 c–e).

Fig. 7 depictes the TEM images of SAPO 34 zeolite prepared for 96 h and 120 h. From the figure it is clear that after 96 h (Fig. 7a), some AlPO phase, rectangular plate like shape was formed. SAED picture of the same area is shown in Fig. 7b confirm the poly crystalline nature. Fig. 7c and d shows the cubical chabazite structure and corresponding SAED image after 120 h synthesis.

Poly crystalline zeolite membrane contains defects i.e. inter-crystalline pathway which is also called non-zeolitic pores. The synthesis procedure, type of zeolite and heat treatment condition affect the concentration of defect. The transport mechanism of gas molecules through non-zeolitic pores is difficult and it is difficult to quantify because the pore size of these non-zeolitic pores are not well defined. Usually non-zeolitic pores are larger than zeolitic pores. Presences of non-zeolitic pores reduce the selectivity of the gases.

In our previous work [17], we have reported that the main sources of non zeolitic pores are resulted from cracks and defects of the membrane layer.

The main cause of the crack was due to the lack of good adherence between zeolite layer and substrate layer.

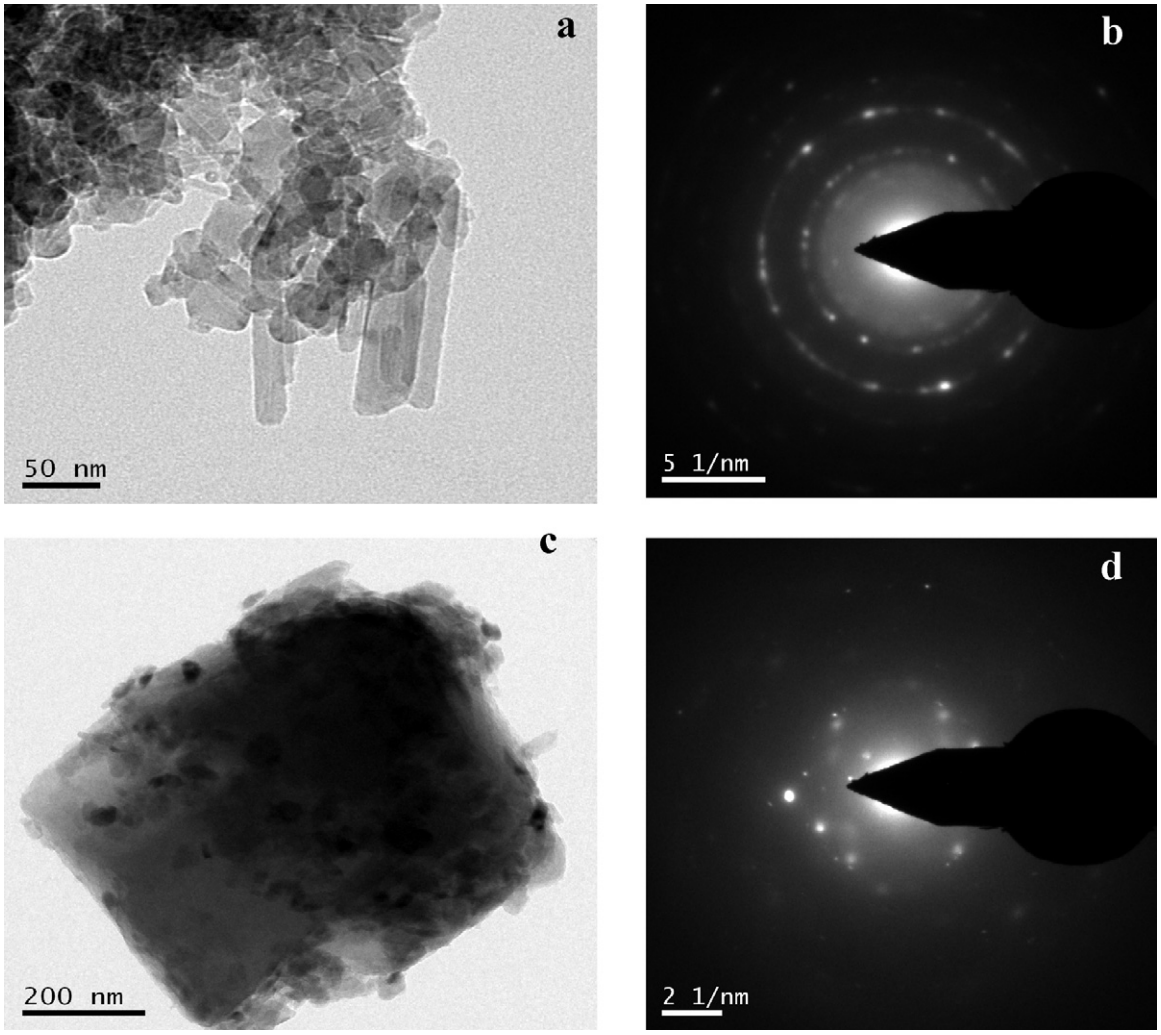

Fig. 7. TEM image and SAED pattern of SAPO 34 powders, synthesized for (a, b) 96 h, (c, d) 120 h.

Considering this fact and to obtain a crack free membrane layer on the substrate, proper seeding on the surface is desirable. Fig. 8 shows the seeded substrate along with its EDAX analysis

However XRD and SEM can only indicate whether a continuous membrane was formed or not on the support, but cannot confirm the quality of zeolite membrane. The quality of zeolite membrane can only be evaluated by gas permeation properties of the membrane. It is well known that performance of a membrane will increases with decreasing defects.

The permeation of CO_2 and H_2 was measured at room temperature directly after calcining the membrane.

The permeation of gas through the micropores of the zeolite can be explained quantitatively by adsorption–diffusion mechanism, where the permeated flux is expressed as the diffusion rate through the micropores between the two sides of the membrane [18]. The diffusion rate becomes significantly smaller where the kinetic diameter of the gas becomes larger than the size of the zeolitic pores due to the molecular sieving effect. So the single gas permeation depends on the kinetic diameter of the gases. Among CO_2 and H_2, kinetic diameter of CO_2 is more than that of H_2. But, in case of SAPO 34 membrane the gas flux of CO_2 is more than that of H_2 as described in Table 2. It indicates that flux was controlled by adsorption coverage not by molecular sieving effect. H_2 fluxes increases with increasing feed pressure as diffusion rate increases. But for CO_2, flux rate decreases with increasing pressure. And ultimately at higher pressure 500 kPa, the flux of CO_2 and H_2 became more or less same. Because at high pressure, CO_2 adsorb more strongly on SAPO 34 zeolite membrane surface than H_2 and the rate of desorption of CO_2 from the membrane surface also decreased. As a result flux rate decreased. Table 3 shows the permeability results of CO_2 and H_2 through SAPO 34 zeolite membranes. At comparatively lower pressure, 200–500 kPa, the permeance value of hydrogen gas increased progressively but in case of CO_2, initially the permeance value at 200–400 kPa increased and then at 500 kPa the permeance value decreased drastically. The permeance properties of the mixture gases were different from single gases. Fig. 9 depicts the permeation properties of single gas and mixture gases of CO_2 and H_2. From figure it is clear that in contrary to single gas permeation properties, mixture gas behaves differently. In

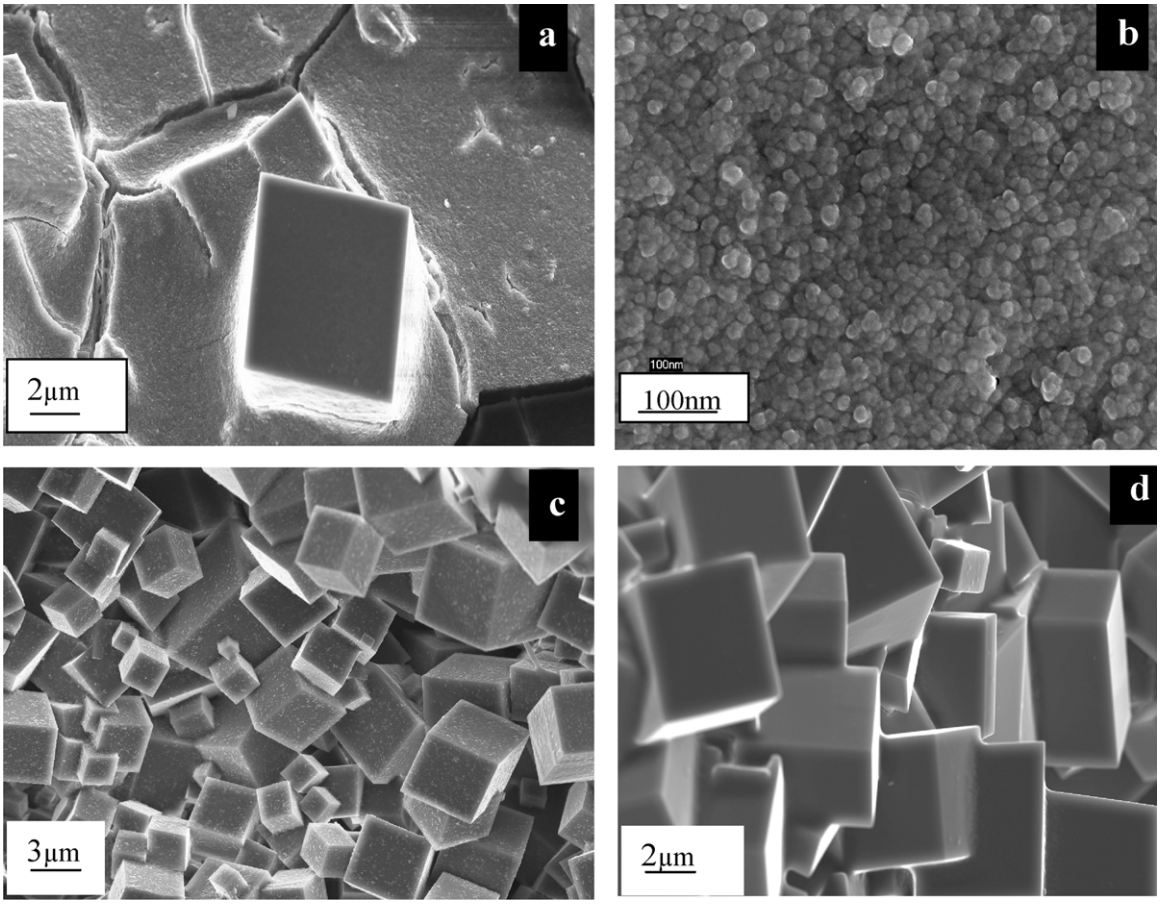

Fig. 8. FESEM micrograph of SAPO 34 membrane seeded substrate synthesized for (a) 48 h, (b) 72 h, (c) 110 h, (d) 120 h.

mixture larger molecule CO_2 permeates faster than H_2 molecule. In case of SAPO 34 membrane, both the molecules have smaller kinetic diameter than zeolite pore size. But in case of competitive adsorption CO_2 adsorbs more strongly, and it hinders the adsorption of H_2 gases. As CO_2 adsorbed preferentially it also desorbs and diffuses earlier than that of H_2. As a results, the flux rate of CO_2 is more than that of H_2 in case of gas mixture. The H_2/CO_2 selectivity was changed from 0.85 to 2.67 which is higher than reported values [19,20]. In case of H_2 and CO_2, the separation is controlled by competitive adsorption and diffusion. The combine effect of these two determines the ultimate selectivity.

Table 2
Change of flux of H_2 and CO_2 single gas at different feed pressures.

Temperature (°C)	Pressure (kPa)	Flux (mol/m^2/s)	
		H_2	CO_2
30	200	0.132	0.182
30	300	0.176	0.269
30	400	0.231	0.324
30	500	0.315	0.324

Table 3
Room temperature single gas permeation for H_2 and CO_2.

Temperature (°C)	Pressure (kPa)	Permeance ($\times 10^7$ mol/m^2 s Pa)		Selectivity
		H_2	CO_2	
30	200	10.23	12.0	0.85
30	300	22.5	23.2	0.96
30	400	29.5	27.5	1.07
30	500	40.1	15.0	2.67

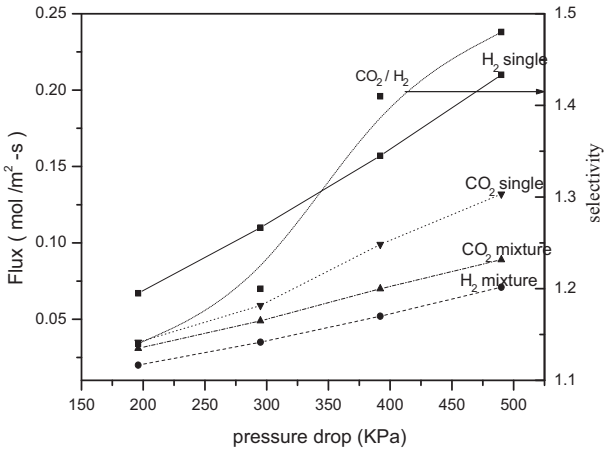

Fig. 9. CO_2 and H_2 fluxes for single gas and CO_2 and H_2 mixture (50/50) at 30 °C as a function of pressure drop.

4. Conclusion

SAPO 34 membranes were synthesized on clay–alumina tubular support. The membrane in this study was synthesized by ex situ hydrothermal technique. Gradual formation of SAPO 34 from initial gel followed the path of cluster formation followed by segregation and crystallization.

Crystallization of SAPO 34 membrane showed that at initial stages, ''pseudo crystalline'' phases were formed which are morphologically similar to SAPO 34 phase. But in the next stage, by rearrangement and gel conversion process zeolite phase was formed. Maximum Si incorporation was done at this stage. IR studies of different stages of membrane formation showed that only after 120 h, D-6 ring was formed which indicates the complete formation of CHA type SAPO 34 structure. Silicon incorporation in $AlPO_4$ phase completes the formation of SAPO 34 structure. Single gas permeation studies showed that selectivity (permeability ratio) of the permeance increases with increasing feed pressure. In case of mixture gases, permeance behavior is different from single gas permeability. For mixture gases, the permeance of H_2 was lower may be due to lower adsorbed concentration of gas on membrane surface. The CO_2 and H_2 mixture selectivity may be increased by changing surface property of the SAPO 34 membrane so that degree of absorption and diffusion of CO_2 may be increased.

Acknowledgements

The authors would like to thank CSIR, India for financial support in the project no. SIP 0023 and also thankful to Dr. I. Manna, Director, CGCRI for his kind permission to publish the research work.

References

[1] S. Li, J.G. Martinek, J.K. Falconer, R.D. Noble, T.Q. Gardner, High pressure CO_2/CH_4 separation using SAPO 34 membrane, Ind. Eng. Chem. Res. 44 (2005) 3220–3228.
[2] M.A. Djieugoute, A.M. Prakash, L. Kevan, Catalytic study of methanol-to-olefins conversion in four small-pore silicoaluminophosphate molecular sieves: influence of the structural type, nickel incorporation, nickel location, and nickel concentration, J. Phys. Chem. B 104 (2000) 6452–6461.
[3] M. Gallo, T.M. Neoff, M.C. Mitchel, Selectivities for binary mixtures of hydrogen/methane and hydrogen/carbon di oxide in silicate and ETS 10 by Grand Canonical Monte Carlo technique, Fluid Phase Equilib. 247, 135 (1–2) (2006) 135–142.
[4] M. Hong, S. Li, J.L. Falconer, R.D. Noble, Hydrogen purification using a SAPO 34 membrane, J. Membr. Sci. 307 (2008) 277–283.
[5] M. Freemantle, Membrane for gas separation, Chem. Eng. News 83 (2005) 49–57.
[6] D.W. Breck, Zeolite Molecular Sieves, Wiley, New York, 1974.
[7] T.M. Neoff, R.J. Spontak, C.M. Aberg, Membranes for hydrogen purification: an important step towards a hydrogen based economy, MRS Bull. 31 (2006) 735–740.
[8] X. Xu, W. Yang, J. Liu, L. Lin, Synthesis of a high performance NaA zeolite membrane by microwave heating, Adv. Mater. 12 (3) (2000) 195–198.
[9] G. Yang, X. Zhang, S. Liu, K.L. Yeung, J. Wang, A novel method for the assembly of nano-zeolite crystals on porous stainless steel microchannel and then zeolite film growth, J. Phys. Chem. Solids 68 (2007) 26–31.
[10] A. Huang, Y.S. Lin, W. Yang, Synthesis and properties of A-type zeolite membranes by secondary growth method with vacuum seeding, J. Membr. Sci. 245 (2004) 41–51.
[11] L.C. Boudreau, T. Tsapatsis, A highly oriented thin film zeolite A, Chem. Mater. 9 (1997) 1705–1707.
[12] M. Tsapatsis, M.C. Lovallo, T.O. Kubo, M.E. Davis, M. Sadakata, Characterization of zeolite L nanoclusters, Chem. Mater. 7 (1995) 1734–1736.
[13] M.C. Lovallo, M. Tsapatsis, Preferentially oriented submicron silicalite membranes, AIChE J. 42 (1996) 3020–3031.
[14] X.C. Xu, W.S. Yang, J. Liu, L.W. Lin, Synthesis and perfection evaluation of NaA zeolite membrane, Sep. Purif. Technol. 25 (2001) 475–486.
[15] T.C Bowen1, R.D. Noble, J.L. Falconer, Fundamentals and applications of pervaporation through zeolite membranes, J. Membr. Sci. 245 (2004) 1–33.
[16] S. Ashtekar, S.V.V. Chilukuri, D.K. Chakrabarty, Small-pore molecular sieves SAPO-34 and SAPO-44 with chabazite structure a study of silicon incorporation, J. Phys. Chem. 98 (1994) 4878–4883.
[17] Nandini Das, Effect of cellulose buffer layer on synthesis and gas permeation properties of NaA zeolite membrane, Ceram. Int. 36 (2010) 1193–1199.
[18] L.C. Boudreau, J.A. Kuck, M. Tsapatsis, Deposition of oriented zeolite A films: in situ and secondary growth, J. Membr. Sci. 152 (1999) 41–59.
[19] J.C. Poshusta, V.A. Tuan, E.A. Pape, R.D. Noble, J.L. Falconer, Separation of light gas mixtures using SAPO 34 membranes, AIChE J. 46 (4) (2000) 779–789.
[20] S. Li, C.Q. Fan, High flux SAPO 34 membrane for CO_2/N_2 separation, Ind. Eng. Chem. Res. 49 (9) (2010) 4399–4404.